

Regional Rescue of SCA1 Phenotypes by $14-3-3\epsilon$ Haploinsufficiency in Mice Underscores Complex Pathogenicity in Neurodegeneration

Paymaan Jafar-Nejad, MD^{1,4}; Christopher S. Ward¹;
Ronald Richman, BS³; Harry T. Orr, PhD⁵;
and Huda Y. Zoghbi, MD^{1,2,3,4}

¹Department of Molecular and Human Genetics

²Department of Neuroscience

³Howard Hughes Medical Institute
Baylor College of Medicine
Houston, Texas

⁴Jan and Dan Duncan Neurological Research Institute
Texas Children's Hospital
Houston, Texas

⁵Department of Laboratory Medicine and Pathology, Department of
Biochemistry, and Institute of Human Genetics
University of Minnesota
Minneapolis, Minnesota

Introduction

Neurodegenerative “proteinopathies,” such as Parkinson’s, Alzheimer’s, and Huntington’s diseases, often involve disruptions of protein homeostasis resulting from altered protein interactions, functions, or degradation (Liu et al., 2002; Giorgini and Muchowski, 2005; Yamin et al., 2008). This disruption may be most readily appreciated in the polyglutamine diseases, a group that includes nine different conditions caused by an expansion of a translated CAG tract (polyQ) in distinct genes (Gatchel and Zoghbi, 2005). Early investigations sought to understand the toxicity mediated specifically by the polyQ peptides (Nagai et al., 1999), which do indeed exert widespread neuronal toxicity when expressed on their own. Research during the past decade, however, has demonstrated that other domains in the polyQ-containing proteins are necessary for the disease-specific patterns of neurodegeneration. For example, serine 13 and 16 are important for huntingtin pathogenesis (Gu et al., 2009), and mutations in caspase cleavage sites block nuclear localization and toxicity of polyQ-expanded huntingtin and androgen receptor (Ellerby et al., 1999; Graham et al., 2006). In the case of expanded Atxn1, either mutation of the nuclear localization signal (Klement et al., 1998), deletion of the AXH domain (de Chiara et al., 2005; Tsuda et al., 2005), or a serine-to-alanine substitution at residue 776 prevents the appearance of SCA1 phenotypes in mice (Emamian et al., 2003).

SCA1 usually causes onset of slowly progressive gait ataxia in midlife to late life, eventually impairing overall motor coordination and producing dysarthria, hypometric saccades, weight loss, respiratory dysfunction, and premature death (Zoghbi and Orr, 1995; Sriranjini et al., 2010). Cerebellar Purkinje cells are the first to be affected, which accounts for the presenting ataxia, but the pons and brainstem are also prominently involved. *Scal* knock-in mice, which bear a CAG expansion of 154Q at the endogenous locus (*Scal*^{154Q/+}) (Watase et al., 2002), recapitulate the features of human SCA1: from ataxia and motor dysfunction to weight loss, progressive Purkinje cell degeneration, and premature death (Watase et al., 2002). Using these mice, we have shown that the pathogenicity of mutant Atxn1 derives not from interactions with novel proteins but from alterations in its interactions with various native protein partners (Chen et al., 2003; Lam et al., 2006; Bowman et al., 2007; Lim et al., 2008). In particular, the toxicity of mutant Atxn1 derives from its incorporation into its large (1.5–3 MDa) native complexes: the S776A substitution, which does not exert toxicity, prevents mutant Atxn1 from incorporating into its large complexes (Emamian et al., 2003; Lam et al., 2006);

also, displacing mutant Atxn1 from its large native complexes by overexpressing its paralogue, Atxn1-like, suppresses the phenotypes of the *Scal*^{154Q/+} mice (Bowman et al., 2007). These findings highlight the importance of Atxn1 large native complexes in SCA1 pathophysiology *in vivo*.

One group of protein interactors is of particular interest for pathogenesis studies: those whose interaction with Atxn1 requires phosphorylation at S776 and is enhanced by the expansion of the polyglutamine tract (Chen et al., 2003). The 14-3-3 proteins, among the first identified Atxn1 interactors, fall into this category. Widely expressed in eukaryotic cells (Takahashi, 2003), these proteins are highly conserved — from yeast to mammals (Aitken et al., 1992); they bind to phosphopeptide motifs in a variety of cellular proteins and can protect their target proteins from proteolysis and dephosphorylation (Muslin et al., 1996). Consistent with this function, we previously found that overexpression of 14-3-3 ϵ stabilizes Atxn1 in cells and increases the toxicity of Atxn1[82Q] in the fly model (Chen et al., 2003). We therefore hypothesized that removing one copy of 14-3-3 might mitigate the disease phenotype. To select a particular isoform of 14-3-3 for genetic interaction studies was not exactly straightforward: several of the seven 14-3-3 isoforms found in mammals (Tzivion and Avruch, 2002), including ϵ , ζ , η , β , and γ , interact with Atxn1 (Chen et al., 2003). The interaction of the ϵ and ζ isoforms with Atxn1 was identified primarily by immunoprecipitation of Atxn1[82Q], whereas the β and ϵ isoforms were the most frequently identified partners in a yeast two-hybrid screen for Atxn1 interactors (Chen et al., 2003). Sequence similarity among 14-3-3 isoforms suggests that some of them are probably functionally redundant (Aitken et al., 1992); thus, the effects of deleting one copy of one isoform might be masked by the presence of other isoforms. The fact that 14-3-3 ϵ ^{-/-} mice die at birth, however, indicates that this isoform has distinct, nonredundant functions (Toyo-oka et al., 2003). We therefore chose 14-3-3 ϵ (also known as Ywhae) to breed with the *Scal*^{154Q/+} mice.

To our surprise, we found that 14-3-3 ϵ haploinsufficiency strongly rescued motor phenotypes but not other aspects of SCA1 that appear unrelated to the cerebellum. This finding led us to investigate the biochemical correlation of such rescue to reveal region-specific differences in Atxn1 complexes. The findings from this study demonstrate that different pathogenic processes can take place in different vulnerable brain regions, highlighting the complexity of mechanisms underlying neurodegeneration in a single disorder.

Results

Diminishing *14-3-3ε* rescues the SCA1 motor phenotype and cerebellar neuropathology

Atxn1 protein level was clearly reduced in crude cerebellar extracts from *14-3-3ε*^{+/-} mice (Fig. 1A). We conclude that *14-3-3ε* stabilizes Atxn1 protein *in vivo* in mouse cerebellum. To determine whether *14-3-3ε* gene dosage affects the SCA1 phenotype, we crossed *14-3-3ε*^{+/-} animals with the *Sca1*^{154Q/+} mice and assessed their motor coordination on the accelerating rotarod at 7 weeks of age and their general motor function with the open-field activity (OFA) test at 20 weeks of age. The *Sca1*^{154Q/+}; *14-3-3ε*^{+/+} animals (from here on referred to as *Sca1*^{154Q/+} mice), as expected, showed significantly worse performance both on the rotarod and OFA than their wild-type (Wt) littermates ($p < 0.001$ and $p < 0.05$, respectively) (Fig. 1B,C).

Removing one copy of *14-3-3ε* in *Sca1*^{154Q/+} mice, however, rescued both rotarod and OFA phenotypes (Fig. 1B,C).

Would *14-3-3ε* haploinsufficiency noticeably affect the cerebellar neuropathology of *Sca1*^{154Q/+} mice? Although Purkinje cell (PC) loss is prominent in human patients, in adult *Sca1*^{154Q/+} mice only about 10% of PCs are lost; dendritic arborization is the most notable pathologic sign (Watase et al., 2002; Bowman et al., 2007). At 32–35 weeks of age, *14-3-3ε* haploinsufficiency rescued PC dendritic phenotype ($p < 0.005$) (Fig. 1D). The complexity of dendritic arbors and PC soma in the *Sca1*^{154Q/+}; *14-3-3ε*^{+/-} mice, as examined by immunofluorescent confocal imaging, resembled that of Wt littermates (Fig. 1E), and there was no PC loss normally observed in adult *Sca1*^{154Q/+} animals ($p < 0.0001$) (Fig. 1E,F). Reducing *14-3-3ε* thus completely rescued the ataxia and cerebellar pathology caused by polyglutamine-expanded Atxn1.

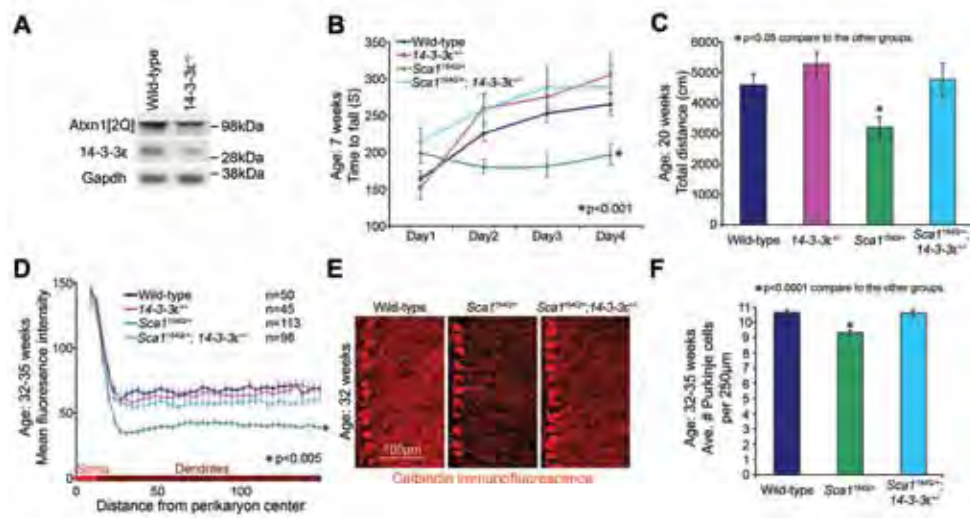


Figure 1. Haploinsufficiency of *14-3-3ε* rescues SCA1 cerebellar phenotype. **A**, Western blot for *14-3-3ε*, Wt Ataxin1 (Atxn1[2Q]), and the control Gapdh in cerebellar lysates. **B**, Accelerating rotarod; the average of 4 trials per day per animal (\pm SEM); (>19 animals/group); ANOVA; *14-3-3ε* haploinsufficiency rescues incoordination of *Sca1*^{154Q/+} mice ($p < 0.001$) to Wt and *14-3-3ε*^{+/-} littermates ($p = 0.27$ and $p = 0.47$, respectively). **C**, OFA test; the average total distance traveled by each animal in 30 min (\pm SEM); (>19 animals/group); ANOVA; *14-3-3ε* heterozygosity restores activity level of *Sca1*^{154Q/+} mice to level of Wt or *14-3-3ε*^{+/-} littermates ($p = 0.78$ and $p = 0.46$ respectively). **D**, Quantitative calbindin immunofluorescence of cerebellar Purkinje cell dendrites. Mean fluorescence intensity of the indicated number of optical rectangular subsections from the crus/II folia of 32- to 35-week-old animals ($n = 3$) was plotted as distance from perikaryon center (\pm SEM); ANOVA; *14-3-3ε* heterozygosity rescues the *Sca1*^{154Q/+} loss of dendritic arborization phenotype ($p < 0.005$); there were no significant differences between double mutants and their Wt or *14-3-3ε*^{+/-} littermates ($p = 0.18$ and $p = 0.47$, respectively). **E**, Representative confocal images showing Purkinje cell morphology from the crus/II folia of littermate-matched 32-week-old animals. Scale bar, 100 μ m. **F**, Quantification of Purkinje cell rescue, graphed as the average number of soma per 250 μ m length (\pm SEM) along the Purkinje cell layer in individual confocal optical sections ($p < 0.0001$). (Wt: 807 neurons along 19,000 μ m in $n = 18$ optical sections; *Sca1*^{154Q/+}: 867 neurons along 23,250 μ m in $n = 23$ optical sections; *Sca1*^{154Q/+}; *14-3-3ε*^{+/-}: 858 neurons along 20,250 μ m in $n = 20$ optical sections).

14-3-3ε haploinsufficiency reduces incorporation of mutant Atxn1 into its large native complexes

The pathogenicity of mutant Atxn1 correlates directly with its level: *Sca1*^{154Q/154Q} and homozygote transgenic (B05) mice show significantly more severe phenotypes than their heterozygote littermates (Burright et al., 1995; Watase et al., 2002). Our *in vivo* data strongly suggest that the stability of the Wt Atxn1 depends, at least in part, on the presence of 14-3-3ε at its physiological levels (Fig. 1A). 14-3-3ε haploinsufficiency might therefore rescue the SCA1 cerebellar phenotypes by diminishing the levels of mutant Atxn1. Western blot analysis on crude cerebellar extracts showed that the *Sca1*^{154Q/+}; 14-3-3ε^{+/-} mice had significantly lower levels of both expanded Atxn1 and Wt Atxn1 compared with their *Sca1*^{154Q/+} littermates (20% and 30%, respectively; *p* < 0.05) (Fig. 2A–C).

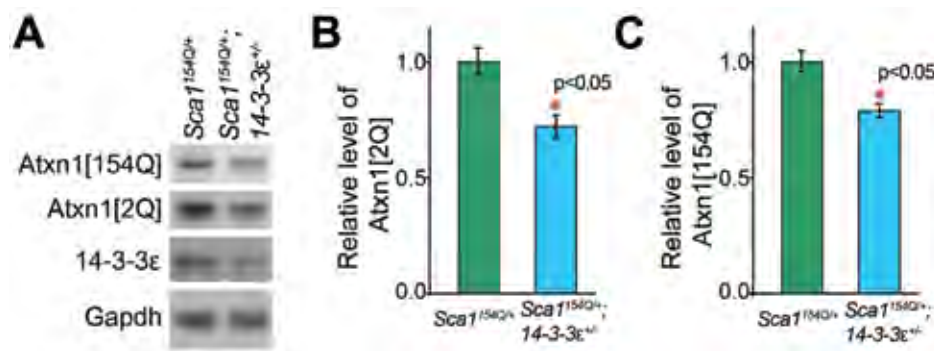


Figure 2. Haploinsufficiency of 14-3-3ε decreases the levels of both Wt and expanded Ataxin1 in *Sca1*^{154Q/+} mice. A–C, Western blot analysis of mouse cerebellar extracts (genotypes indicated), using antisera to 14-3-3ε, Ataxin1 (2Q and 154Q), and Gapdh (control). The average level (±95% confidence interval) of Atxn1[2Q] and Atxn1[154Q] proteins in *Sca1*^{154Q/+}; 14-3-3ε^{+/-} relative to levels in *Sca1*^{154Q/+} extracts is illustrated in panels B and C, respectively (*n* = 6).

Given the importance of the Atxn1 large complexes in SCA1 pathogenesis, we next compared the formation of small and large Atxn1 complexes in *Sca1*^{154Q/+}; 14-3-3ε^{+/-} mice and their *Sca1*^{154Q/+} littermates by analyzing the elution profiles of Atxn1[2Q] and Atxn1[154Q] in size-exclusion chromatography fractions of mouse cerebellar protein extracts (Fig. 3A). Quantification of the Atxn1 elution profiles showed that the ratio of large to small Atxn1[154Q] (but not Atxn1[2Q]) protein complexes in the *Sca1*^{154Q/+}; 14-3-3ε^{+/-} extracts was significantly lower than in the *Sca1*^{154Q/+} extracts (*p* = 0.011) (Fig. 3B–E). These data suggest that, in addition to reducing Atxn1 levels, heterozygosity for

14-3-3ε decreases the incorporation of Atxn1[154Q] into the large complexes, some of which are known to be toxic in the cerebellum.

Heterozygosity for the 14-3-3ε null allele does not rescue all SCA1 phenotypes

Despite the dramatic rescue of the motor phenotypes and cerebellar pathology, 14-3-3ε haploinsufficiency did not mitigate the premature death or weight loss — phenotypes that are less likely to derive from cerebellar dysfunction (data not shown). In fact, the precise cause of death in *Sca1*^{154Q/+} mice has never been established. Close observation of several *Sca1*^{154Q/+} mice has shown that they are able to eat even a few hours before their death; postmortem studies of several *Sca1*^{154Q/+} mice found food in the stomach and feces in the colon, so the animals do not starve to death. Aside from overall brain atrophy, however, we were unable to detect specific neuropathology in any other brain region than the cerebellum (Watase et al., 2002).

Patients with SCA1 suffer from pulmonary dysfunction that worsens over time and likely contributes to their death. Using spirometric tests, Sriranjini et al. (2010) found evidence of

restrictive lung dysfunction, upper airway obstruction, and reduced muscle strength that could have arisen from a combination of factors, including pulmonary dormancy, poor respiratory muscle coordination, and bulbar dysfunction (Sriranjini et al., 2010). We therefore wondered if *Sca1*^{154Q/+} mice, which replicate so many aspects of the human disease, might also suffer from respiratory dysregulation. Using unrestrained whole-body plethysmography, we assessed the basic respiratory pattern in *Sca1*^{154Q/+} mice. At 5 weeks of age, the *Sca1*^{154Q/+} mice did not differ significantly from their Wt littermates (*p* = 0.16); however, by 33 weeks of age, both *Sca1*^{154Q/+} and *Sca1*^{154Q/+}; 14-3-3ε^{+/-} mice showed significantly more shallow,

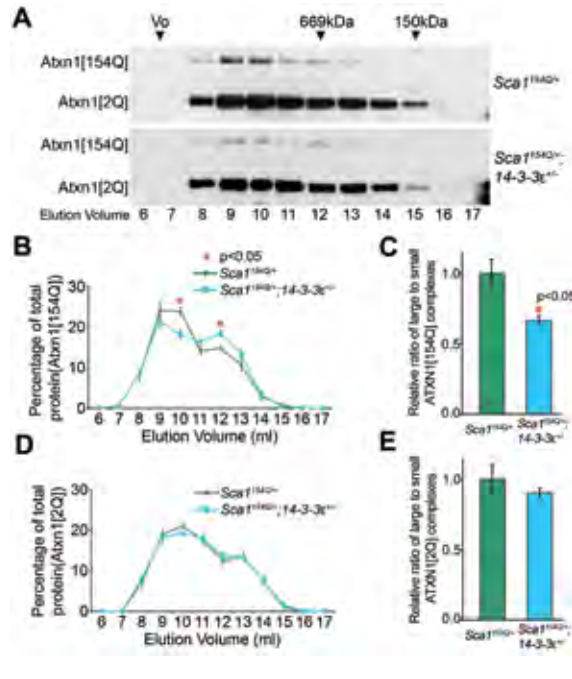


Figure 3. Haploinsufficiency of *14-3-3ε* shifts mutant Atxn1 from its large to its small complexes. **A**, Representative Western blots of size exclusion chromatography fractions from mouse cerebellar extracts analyzed for Atxn1[2Q] and Atxn1[154Q]. The column void volume (V_0) and elution volume (ml) of each collected fraction are indicated. **B**, The Atxn1[154Q] gel filtration elution profiles of cerebellar extract plotted as the percentage of Atxn1[154Q] (mean \pm SEM) in each fraction (amount per fraction compared with total amount of Atxn1[154Q] in all fractions) from independent extracts. **C**, Large (in the peak elution fractions, 9 and 10 ml) to small (in the peak elution fraction, 12 and 13 ml) Atxn1[154Q] complexes (mean \pm SEM). **D**, The Atxn1[2Q] gel filtration elution profiles of cerebellar extract plotted ($n = 4$). **E**, Large to small Atxn1[2Q] complexes (mean \pm SEM) ($n = 4$).

rapid respiration than their Wt littermates ($p < 0.01$) (data not shown). The respiratory phenotype of these mice, which has not been reported before, worsens with time, becoming most severe just prior to death. Suffice it to say, *14-3-3ε* haploinsufficiency does not appear to rescue phenotypes arising from parts of the nervous system outside of the cerebellum. The selective rescue of the SCA1 phenotypes in our genetic interaction raised the possibility of a distinct mechanism limited to the cerebellum.

Atxn1 complex formation differs between the cerebellum and the brainstem

To investigate whether the biochemical changes we discovered are as specific to the cerebellum as the phenotypic rescue, we examined the brainstem.

Not only is this brain region severely affected in SCA1, but bulbar dysfunction may well be involved in the nonrescued respiratory phenotype described above. To compare the biochemical studies on the brainstem with cerebellar findings, we had to answer two important questions: (1) whether *14-3-3ε* is expressed in the brainstem and (2) whether *14-3-3ε* and Atxn1 interact in the brainstem. Immunoblot analysis of cerebellar and brainstem lysates showed that *14-3-3ε* levels are the same in both regions (Fig. 4A). This is consistent with previous reports that *14-3-3ε* is ubiquitous in the brain (Baxter et al., 2002; Umahara et al., 2007). We then confirmed that Atxn1 co-immunoprecipitated with *14-3-3ε* in the brainstem (Fig. 4B). These results show that the reason for lack of rescue of a phenotype arising from the brainstem is neither lack of *14-3-3ε* expression nor lack of its interaction with Atxn1 in the brainstem.

A closer look at the protein levels in the extracts from the cerebellum and brainstem of *Sca1*^{154Q/+} mice revealed that the level of Wt Atxn1 in the brainstem of the *Sca1*^{154Q/+} mice was noticeably lower than in the cerebellum, but that the level of expanded Atxn1[154Q] was the same in both regions (Fig. 4A). The ratio of mutant to Wt Atxn1 in the brainstem was thus two to three times greater than in the cerebellum (Fig. 4C), which would likely make *14-3-3ε* heterozygosity less effective in mitigating brainstem degeneration.

We next quantified Atxn1 levels in crude brainstem extracts from the *Sca1*^{154Q/+}; *14-3-3ε*^{+/-} mice and their *Sca1*^{154Q/+} littermates. We found that, despite a decreased level of *14-3-3ε* in *Sca1*^{154Q/+}; *14-3-3ε*^{+/-} mice, both Wt and mutant Atxn1 levels remained unaltered (data not shown).

Why does *14-3-3ε* haploinsufficiency fail to reduce Atxn1 levels in the brainstem of the *Sca1*^{154Q/+}; *14-3-3ε*^{+/-} mice? The answer cannot involve regional differences in levels of either *14-3-3ε* or expanded Atxn1 (they are the same in both cerebellum and brainstem; Fig. 4A) or lack of Atxn1/*14-3-3ε* interaction in the brainstem (Fig. 4B). We concluded that the mechanism by which *14-3-3ε* stabilizes Atxn1 must take place in the cerebellum but not in the brainstem. We analyzed the size-exclusion chromatography fractions of brainstem extracts from *Sca1*^{154Q/+}; *14-3-3ε*^{+/-} mice and their *Sca1*^{154Q/+} littermates. Unlike the cerebellum, the elution profiles of Atxn1[2Q] and Atxn1[154Q] in the brainstem of these two genotypes showed very similar patterns

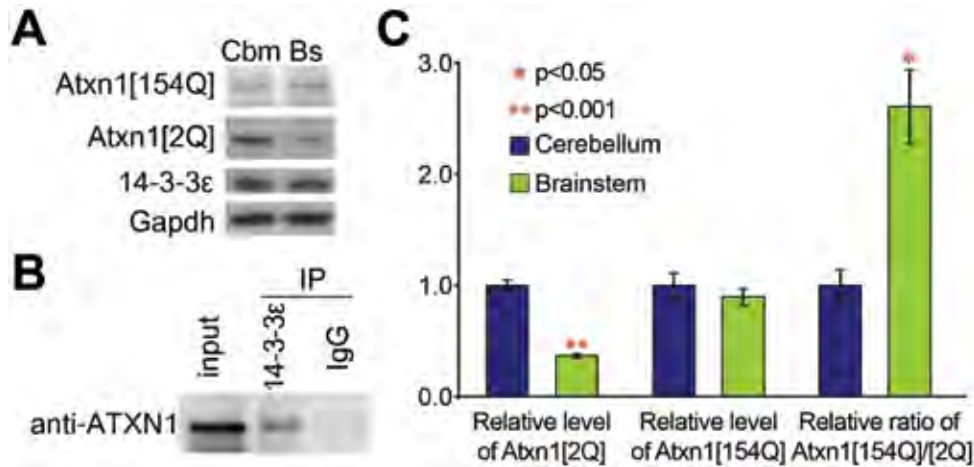


Figure 4. Level of Wt Atxn1, but not 14-3-3ε and expanded Atxn1, is lower in the brainstem. **A**, Western blot analysis of a *Sca1*^{154Q/+} mouse cerebellar (Cbm) and brainstem (Bs) extracts, using antisera to 14-3-3ε, Ataxin1 (2Q and 154Q), and Gapdh (control). **B**, Co-immunoprecipitation of Atxn1 with 14-3-3ε from Wt mouse brainstem extract. **C**, The average levels of Atxn1[2Q] and Atxn1[154Q] proteins in *Sca1*^{154Q/+}; 14-3-3ε^{+/-} relative to levels in *Sca1*^{154Q/+} extracts and relative level of ATXN[154Q] to Atxn1[2Q] in the cerebellum and brainstem are illustrated (±95% confidence interval) (*n* = 6). IgG, immunoglobulin G.

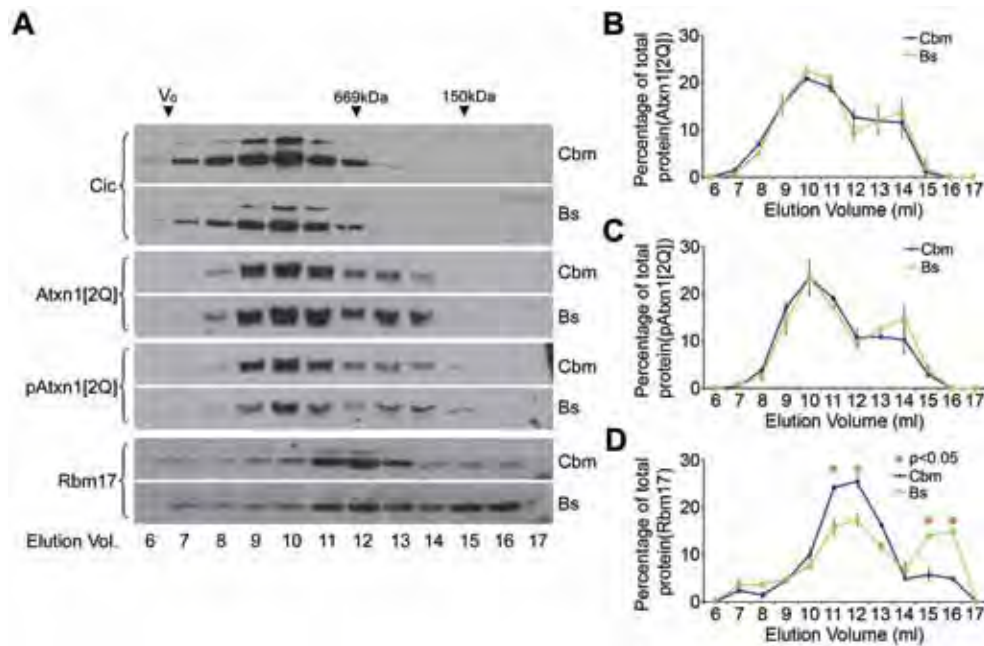


Figure 5. **A**, Representative Western blots from size exclusion chromatography fractions of Wt mouse cerebellar (Cbm) and brainstem (Bs) extracts, analyzed for Capicua (Cic), Atxn1, pAtxn1, and Rbm17. The column void volume (Vo), size exclusion standards thyroglobulin (669 kDa) and alcohol dehydrogenase (150 kDa) and elution volume (ml) of each collected fraction are indicated. **B**, The Atxn1[2Q] gel filtration elution profiles of cerebellar and brainstem extract from a Wt mouse plotted as the percentage of Atxn1[2Q] (mean ± SEM) in each fraction from independent extracts (*n* = 3). **C**, The pAtxn1[2Q] gel filtration elution profiles of cerebellar and brainstem extracts from a Wt mouse plotted as the percentage of pAtxn1[2Q] (mean ± SEM) in each fraction (amount per fraction compared with total amount of pAtxn1[2Q] in all fractions) from independent extracts (*n* = 3). **D**, The Rbm17 gel filtration elution profiles of cerebellar versus brainstem extracts from Wt mouse plotted as the percentage of Rbm17 (mean ± SEM) in each fraction (amount per fraction compared with total amount of Rbm17 in all fractions) from independent extracts (*n* = 4).

NOTES

(data not shown); thus, *14-3-3ε* haploinsufficiency affected the elution profile of mutant Atxn1 in the cerebellum differently from the brainstem, suggesting that Atxn1 forms different native complexes in these two brain regions. To test this hypothesis, we analyzed the elution profiles of Atxn1, Capicua (a prominent native partner of Atxn1), and Rbm17 (a protein that interacts in an S776-dependent manner) (Lim et al., 2008) in size exclusion chromatography fractions of cerebellar and brainstem extracts from Wt mice. The elution profiles of total Atxn1, phospho-Atxn1 (pAtxn1), and Capicua were the same (Fig. 5A–C). The distribution of Rbm17 in the brainstem, however, differed from that in the cerebellum (Fig. 5A,D).

In our *Sca1*^{154Q/+} mouse model, the elution profiles of Capicua and Atxn1[2Q] in the cerebellum and brainstem were similar to those of the Wt mice (Fig. 6A), but the ratio of large to small Atxn1[154Q] protein complexes was much lower ($p < 0.05$) in the brainstem than in the cerebellum (Fig. 6A–C). This suggests that expanded Atxn1 might have different partners that contribute to different toxic complexes in the two brain regions. In agreement with this notion, the elution profile of Rbm17 in *Sca1*^{154Q/+} mice differed from the cerebellum to the brainstem (Fig. 6A,D).

Phosphorylation of Atxn1 at Serine 776 is critical for SCA1 pathogenesis (Chen et al., 2003; Emamian et al., 2003). The distribution of pAtxn1[2Q] and pAtxn1[154Q] in *Sca1*^{154Q/+} cerebellum followed the pattern of total Atxn1, with higher levels in large complexes than in the small ones (Fig. 6A). In *Sca1*^{154Q/+} brainstem, however, the majority of endogenous, Wt pAtxn1 was found in small complexes, and very little was present in large Atxn1 complexes, even though they were enriched for total Atxn1[2Q] (Fig. 6A,E,F).

The very low levels of pAtxn1[154Q] in the brainstem prevented us from evaluating its elution profile (Fig. 6A). Given that the Wt brainstem and cerebellum showed no difference in the distribution of pAtxn1 (Fig. 5A,C), the lack of pAtxn1 in the large

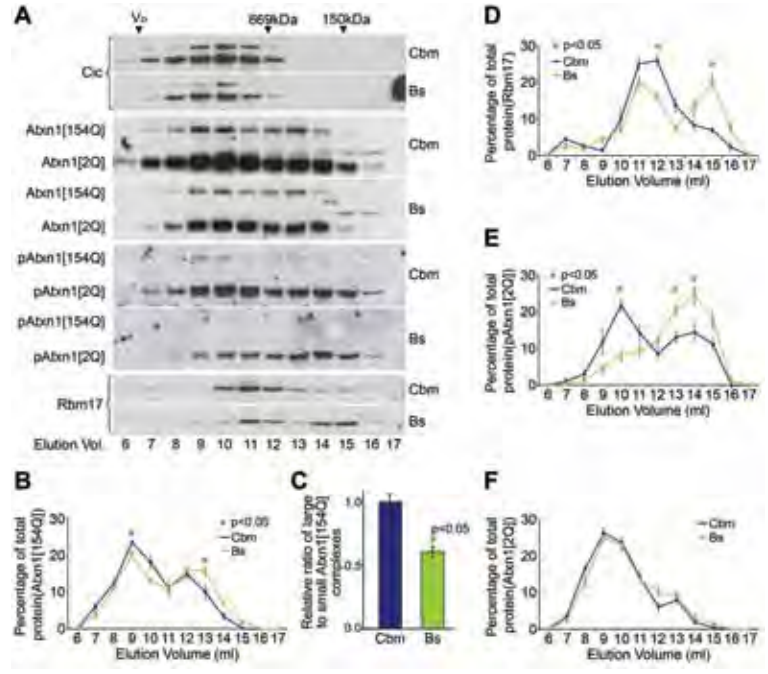


Figure 6. Brainstem (Bs) and cerebellum (Cbm) of *Sca1*^{154Q/+} mice show different distributions of Atxn1[154Q], pAtxn1, and Rbm17. **A**, Representative Western blots of size exclusion chromatography fractions from *Sca1*^{154Q/+} cerebellar and brainstem extracts, analyzed for Capicua (Cic), Atxn1, pAtxn1, and Rbm17. **B**, The Atxn1[154Q] gel filtration elution profiles of cerebellar and brainstem extracts from *Sca1*^{154Q/+} plotted (mean \pm SEM) ($n = 4$). **C**, Large to small Atxn1[154Q] complexes (mean \pm SEM). Significantly less Atxn1[154Q] incorporated into the large complexes in the brainstem than in the cerebellum. Gel filtration elution profiles of **D**, The Rbm17, **E**, pAtxn1[2Q], and **F**, Atxn1[2Q] from cerebellar and brainstem extracts from *Sca1*^{154Q/+} plotted (mean \pm SEM) ($n = 4$).

complexes in the brainstem of *Sca1*^{154Q/+} mice must result from a specific effect of mutant Atxn1 in the brainstem. These data highlight major differences in the distribution pattern of mutant Atxn1 complexes in these two brain regions and suggest that pAtxn1 does not form the same complexes in the brainstem as it does in the cerebellum.

Discussion

A growing body of literature is clarifying the mechanism of SCA1 pathogenesis in the cerebellum. The cerebellar symptoms in SCA1 are the first to appear and the easiest to measure, but the disease progresses to other serious symptoms that do not arise from the cerebellum. In the present study, we show that *14-3-3ε* haploinsufficiency in *Sca1*^{154Q/+} mice rescues SCA1 cerebellar pathology and motor phenotypes. To our knowledge, this is the first dominant genetic suppressor to exhibit such a dramatic effect on the cerebellar phenotype in the *Sca1* mouse model. Our biochemical studies indicate that *14-3-3ε* stabilizes Atxn1; since the level of mutant Atxn1 directly correlates with its

pathogenicity (Burrigh et al., 1995; Lorenzetti et al., 2000; Watase et al., 2002), it seems likely that the reduction in 14-3-3ε alleviates cerebellar pathology at least in part by decreasing levels of mutant Atxn1.

We were surprised to find that 14-3-3ε haploinsufficiency did not rescue all aspects of the phenotype, however: the double mutant mice still lost weight and died prematurely, just like their *Scal*^{154Q/+} littermates. Toyo-oka and colleagues showed that 14-3-3ε^{+/-} mice have mildly disorganized hippocampus and cortical thinning (Toyo-oka et al., 2003). These abnormalities, however, did not interfere with functions we assayed for in this study. We found that 14-3-3ε^{+/-} mice have normal motor coordination and Purkinje cell morphology, normal weight, breathing pattern, and lifespan. Hence, the mild cortical and hippocampal developmental defects in the 14-3-3ε^{+/-} mice are unlikely to be responsible for the nonrescued lifespan phenotype in *Scal*^{154Q/+}; 14-3-3ε^{+/-} mice. In the course of trying to understand the cause of death, we uncovered a respiratory dysfunction that had not been reported previously in the *Scal* knock-in mice but is documented in human patients (Sriranjini et al., 2010). While we were investigating this phenotype, four mice (two *Scal*^{154Q/+} and two *Scal*^{154Q/+}; 14-3-3ε^{+/-} mice) died within two to four days of our last recording. Whether respiratory dysfunction was the immediate cause of death is impossible to ascertain; for that matter, the precise cause of death in human patients has not been firmly established. Aspiration pneumonia is a common (and frequently fatal) complication of end-stage SCA1 (Shiojiri et al., 1999; Ramio-Torrentia et al., 2006). This new unique, quantifiable phenotype in *Scal*^{154Q/+} mice could be used as an outcome measure in future studies of therapeutic interventions.

Notwithstanding the uncertain origins of the nonrescued phenotypes, we decided that examining Atxn1 complex formation in the brainstem, a brain region known to be highly vulnerable in SCA1, might provide insight into the apparently cerebellum-specific rescue. We found that, as previously reported (Baxter et al., 2002), 14-3-3ε is expressed equally in the brainstem and in the cerebellum and that Atxn1 and 14-3-3ε interact in both regions. The haploinsufficiency of 14-3-3ε, however, decreased Ataxin1 levels only in the cerebellum; brainstem levels of both Wt and mutant Atxn1 were unaltered. In exploring the biochemical differences between the cerebellum and the brainstem, we found that some proteins (e.g., Rbm17) have completely different patterns in the two regions. In addition,

the composition of the large Atxn1 complexes differs between the two regions: pAtxn1, which is necessary for 14-3-3/Atxn1 interaction and for the toxicity of mutant Atxn1 in the large complexes in the cerebellum, is not present in the large Atxn1 complexes in the brainstem of *Scal*^{154Q/+} mice.

We also observed that the brainstem of *Scal* mice has lower levels of Wt Atxn1 relative to the expanded protein. It is interesting to note in this context that previous work has shown Wt Atxn1 to exert a protective effect. We have postulated that Wt Atxn1 competes with mutant Atxn1 in binding some protein partners, and thereby reduces the formation of mutant Atxn1 complexes (Lim et al., 2008). The lower levels of Wt Atxn1 (and thus the greater availability of mutant Atxn1 for complex formation in the brainstem) could explain why genetic suppression by 14-3-3ε heterozygosity is ineffective in the brainstem.

Selective neurodegeneration in the context of ubiquitous expression of the disease protein is a common feature of many neurodegenerative diseases (Orr and Zoghbi, 2007); it is a reasonable conjecture that differential vulnerability would be mediated by different protein interactions. What is striking in this study, however, is that we have examined two regions that are both targets of SCA1 and find evidence that pathogenesis in each region differs. In other words, the molecular pathogenesis of neuronal dysfunction within a single disorder can differ among affected brain regions. The finding that the distribution of the mutant protein in its native complexes can vary from one brain region to the next, and that such differences have region-specific effects, underscores the need for in-depth studies on molecular pathogenesis in the multiple cellular contexts typically affected by the disease, with a focus on native complexes. Our data also caution that potential therapeutic modalities should be examined in different brain regions and not generalized to the whole brain from one neuronal group.

Acknowledgments

This paper was published in unabridged form in the journal *Proceedings of the National Academy of Sciences USA* (2011;108:2142-2147). Please refer to the published paper for further description of experimental procedures and supplementary figures. We are grateful to Dr. Anthony Wynshaw-Boris for providing 14-3-3ε^{+/-} mice; the assistance of the mouse phenotyping core facility at Baylor College of Medicine; Sukeshi Vaishnav for mouse genotyping; Dr. Hamed Jafar-Nejad, Dr. Herman Dierick,

NOTES

and the members of the H.Y.Z. laboratories for comments on the manuscript; and V.L. Brandt for editorial input. This work was supported by the National Institutes of Health Grant NS27699 to H.Y.Z., Grant NS022920 to H.T.O., and Grant HD024064 to the Baylor College of Medicine Intellectual and Developmental Disabilities Research Center.

References

- Aitken A, Collinge DB, van Heusden BP, Isobe T, Roseboom PH, Rosenfeld G, Soll J (1992) 14-3-3 proteins: a highly conserved, widespread family of eukaryotic proteins. *Trends Biochem Sci* 17:498-501.
- Baxter HC, Liu WG, Forster JL, Aitken A, Fraser JR (2002) Immunolocalisation of 14-3-3 isoforms in normal and scrapie-infected murine brain. *Neuroscience* 109:5-14.
- Bowman AB, Lam YC, Jafar-Nejad P, Chen HK, Richman R, Samaco RC, Fryer JD, Kahle JJ, Orr HT, Zoghbi HY (2007) Duplication of *Atxn11* suppresses SCA1 neuropathology by decreasing incorporation of polyglutamine-expanded ataxin-1 into native complexes. *Nat Genet* 39:373-379.
- Burright EN, Clark HB, Servadio A, Matilla T, Feddersen RM, Yunis WS, Duvick LA, Zoghbi HY, Orr HT (1995) SCA1 transgenic mice: a model for neurodegeneration caused by an expanded CAG trinucleotide repeat. *Cell* 82:937-948.
- Chen HK, Fernandez-Funez P, Acevedo SF, Lam YC, Kaytor MD, Fernandez MH, Aitken A, Skoulakis EM, Orr HT, Botas J, Zoghbi HY (2003) Interaction of Akt-phosphorylated ataxin-1 with 14-3-3 mediates neurodegeneration in spinocerebellar ataxia type 1. *Cell* 113:457-468.
- de Chiara C, Menon RP, Dal Piaz F, Calder L, Pastore A (2005) Polyglutamine is not all: the functional role of the AXH domain in the ataxin-1 protein. *J Mol Biol* 354:883-893.
- Ellerby LM, Hackam AS, Propp SS, Ellerby HM, Rabizadeh S, Cashman NR, Trifiro MA, Pinsky L, Wellington CL, Salvesen GS, Hayden MR, Bredesen DE (1999) Kennedy's disease: caspase cleavage of the androgen receptor is a crucial event in cytotoxicity. *J Neurochem* 72:185-195.
- Emamian ES, Kaytor MD, Duvick LA, Zu T, Tousey SK, Zoghbi HY, Clark HB, Orr HT (2003) Serine 776 of ataxin-1 is critical for polyglutamine-induced disease in SCA1 transgenic mice. *Neuron* 38:375-387.
- Gatchel JR, Zoghbi HY (2005) Diseases of unstable repeat expansion: mechanisms and common principles. *Nat Rev Genet* 6:743-755.
- Giorgini F, Muchowski PJ (2005) Connecting the dots in Huntington's disease with protein interaction networks. *Genome Biol* 6:210.
- Graham RK, Deng Y, Slow EJ, Haigh B, Bissada N, Lu G, Pearson J, Shehadeh J, Bertram L, Murphy Z, Warby SC, Doty CN, Roy S, Wellington CL, Leavitt BR, Raymond LA, Nicholson DW, Hayden MR (2006) Cleavage at the caspase-6 site is required for neuronal dysfunction and degeneration due to mutant *huntingtin*. *Cell* 125:1179-1191.
- Gu X, Greiner ER, Mishra R, Kodali R, Osmand A, Finkbeiner S, Steffan JS, Thompson LM, Wetzel R, Yang XW (2009) Serines 13 and 16 are critical determinants of full-length human mutant huntingtin induced disease pathogenesis in HD mice. *Neuron* 64:828-840.
- Klement IA, Skinner PJ, Kaytor MD, Yi H, Hersch SM, Clark HB, Zoghbi HY, Orr HT (1998) Ataxin-1 nuclear localization and aggregation: role in polyglutamine-induced disease in SCA1 transgenic mice. *Cell* 95:41-53.
- Lam YC, Bowman AB, Jafar-Nejad P, Lim J, Richman R, Fryer JD, Hyun ED, Duvick LA, Orr HT, Botas J, Zoghbi HY (2006) ATAXIN-1 interacts with the repressor Capicua in its native complex to cause SCA1 neuropathology. *Cell* 127:1335-1347.
- Lim J, Crespo-Barreto J, Jafar-Nejad P, Bowman AB, Richman R, Hill DE, Orr HT, Zoghbi HY (2008) Opposing effects of polyglutamine expansion on native protein complexes contribute to SCA1. *Nature* 452:713-718.
- Liu Y, Fallon L, Lashuel HA, Liu Z, Lansbury PT, Jr. (2002) The *UCH-L1* gene encodes two opposing enzymatic activities that affect alpha-synuclein degradation and Parkinson's disease susceptibility. *Cell* 111:209-218.
- Lorenzetti D, Watase K, Xu B, Matzuk MM, Orr HT, Zoghbi HY (2000) Repeat instability and motor incoordination in mice with a targeted expanded CAG repeat in the *Sca1* locus. *Hum Mol Genet* 9:779-785.
- Muslin AJ, Tanner JW, Allen PM, Shaw AS (1996) Interaction of 14-3-3 with signaling proteins is mediated by the recognition of phosphoserine. *Cell* 84:889-897.

- Nagai Y, Onodera O, Strittmatter WJ, Burke JR (1999) Polyglutamine domain proteins with expanded repeats bind neurofilament, altering the neurofilament network. *Ann NY Acad Sci* 893:192-202.
- Orr HT, Zoghbi HY (2007) Trinucleotide repeat disorders. *Annu Rev Neurosci* 30:575-621.
- Ramio-Torrentia L, Gomez E, Genis D (2006) Swallowing in degenerative ataxias. *J Neurol* 253:875-881.
- Shiojiri T, Tsunemi T, Matsunaga T, Sasaki H, Yabe I, Tashiro K, Nishizawa N, Takamoto K, Yokota T, Mizusawa H (1999) Vocal cord abductor paralysis in spinocerebellar ataxia type 1. *J Neurol Neurosurg Psychiatry* 67:695.
- Sriranjini SJ, Pal PK, Krishna N, Sathyaprabha TN (2010) Subclinical pulmonary dysfunction in spinocerebellar ataxias 1, 2 and 3. *Acta Neurol Scand* 122:323-328.
- Takahashi Y (2003) The 14-3-3 proteins: gene, gene expression, and function. *Neurochem Res* 28:1265-1273.
- Toyo-oka K, Shionoya A, Gambello MJ, Cardoso C, Leventer R, Ward HL, Ayala R, Tsai LH, Dobyns W, Ledbetter D, Hirotsumi S, Wynshaw-Boris A (2003) 14-3-3 ϵ is important for neuronal migration by binding to NUDEL: a molecular explanation for Miller-Dieker syndrome. *Nat Genet* 34:274-285.
- Tsuda H, Jafar-Nejad H, Patel AJ, Sun Y, Chen HK, Rose MF, Venken KJ, Botas J, Orr HT, Bellen HJ, Zoghbi HY (2005) The AXH domain of Ataxin-1 mediates neurodegeneration through its interaction with Gfi-1/Senseless proteins. *Cell* 122:633-644.
- Tzivion G, Avruch J (2002) 14-3-3 proteins: active cofactors in cellular regulation by serine/threonine phosphorylation. *J Biol Chem* 277:3061-3064.
- Umahara T, Uchihara T, Yagishita S, Nakamura A, Tsuchiya K, Iwamoto T (2007) Intranuclear immunolocalization of 14-3-3 protein isoforms in brains with spinocerebellar ataxia type 1. *Neurosci Lett* 414:130-135.
- Watase K, Weeber EJ, Xu B, Antalffy B, Yuva-Paylor L, Hashimoto K, Kano M, Atkinson R, Sun Y, Armstrong DL, Sweatt JD, Orr HT, Paylor R, Zoghbi HY (2002) A long CAG repeat in the mouse *Scal* locus replicates SCA1 features and reveals the impact of protein solubility on selective neurodegeneration. *Neuron* 34:905-919.
- Yamin G, Ono K, Inayathullah M, Teplow DB (2008) Amyloid beta-protein assembly as a therapeutic target of Alzheimer's disease. *Curr Pharm Des* 14:3231-3246.
- Zoghbi HY, Orr HT (1995) Spinocerebellar ataxia type 1. *Semin Cell Biol* 6:29-35.